PHYSICAL REVIEW D **86,** 095024 (2012)

Allowed slepton intergenerational mixing in light of light element abundances

Kazunori Kohri,[1,2] Shingo Ohta,[3] Joe Sato,[3] Takashi Shimomura,[4,5] and Masato Yamanaka[1]

[1]*Theory Center, Institute of Particle and Nuclear Studies, KEK (High Energy Accelerator Research Organization), 1-1 Oho, Tsukuba 305-0801, Japan*

[2]*The Graduate University for Advanced Studies (Sokendai), 1-1 Oho, Tsukuba 305-0801, Japan*

[3]*Department of Physics, Saitama University, Shimo-okubo, Sakura-ku, Saitama 338-8570, Japan*

[4]*Department of Physics, Niigata University, Niigata 950-2181, Japan*

[5]*Max-Planck-Institut für Kernphysik, Saupfercheckweg 1, 69117 Heidelberg, Germany*

(Received 5 September 2012; published 19 November 2012)

We studied allowed region on the intergenerational mixing parameters of sleptons from a viewpoint of big-bang nucleosynthesis in a slepton-neutralino coannihilation scenario. In this scenario, ^{7}Li and ^{6}Li problems can be solved by considering exotic reactions caused by bound-state effects with a long-lived slepton. Light element abundances are calculated as functions of the relic density and lifetime of the slepton which considerably depend on the intergenerational mixing parameters. Compared with observational light element abundances, we obtain allowed regions on the intergenerational mixing. Ratio of selectron component to stau component, c_e, is allowed in $2 \times 10^{-11} \lesssim c_e \lesssim 2 \times 10^{-9}$ with solving both the ^{7}Li and ^{6}Li problems. Similarly, the ratio for smuon, c_μ, is allowed in $c_\mu \lesssim 5 \times 10^{-5}$ for mass difference between slepton and neutralino, which is smaller than muon mass, and $c_\mu \lesssim 2 \times 10^{-10}$ for the mass difference in range between muon mass and 125 MeV. We also discuss collider signatures of the slepton decays. We find characteristic double peaks in momentum distribution of event number of the slepton decays with allowed mixing parameters. Discoveries of the double peaks at future collider experiments should confirm our scenario.

DOI: 10.1103/PhysRevD.86.095024 PACS numbers: 12.15.Ff, 12.60.Jv, 14.80.Ly, 26.35.+c

I. INTRODUCTION

Long-lived charged massive particles (CHAMP) are predicted in new physics beyond the standard model [1]. Such long-lived CHAMPs induce nonstandard nuclear reactions in big-bang nucleosynthesis (BBN), and drastically change light element abundances [2–21]. By comparing the theoretical predictions with observational data, we can obtain constraints on model parameters relevant with the long-lived CHAMPs. Because the BBN is sensitive to lifetime from 10^{-2} to 10^{12} sec , it should be one of the best tools to check an existence of the long-lived CHAMPs.[1]

The minimal supersymmetric standard model (MSSM) with R-parity conservation is one of the leading candidate providing long-lived CHAMPs. Several MSSM scenarios predict a long-lived stau as the next lightest supersymmetric particle (NLSP). An example is the scenario that the lightest supersymmetric particle (LSP) is gravitino. In this scenario, the interaction of the gravitino LSP with the stau NLSP is suppressed by Planck scale, and hence the stau has longevity [5–7,30–32]. Another example is an axino LSP scenario, in which the decay rate of the stau NLSP is suppressed because of loop processes or a decay constant scale F_a [33–35]. Among such scenarios, the most attractive one is a Bino-like neutralino LSP scenario. The longevity of the stau NLSP is brought by tight mass degeneracy of the stau and the neutralino LSP.

A remarkable feature of this mass-degenerate scenario is to be free from the ^{7}Li problem [36]. The ^{7}Li problem is a discrepancy between the observed abundance of ^{7}Li, e.g., $\mathrm{Log}_{10}(^7\mathrm{Li/H}) = -9.63 \pm 0.06$ [37], and a theoretical one predicted in the standard BBN, $\mathrm{Log}_{10}(^7\mathrm{Li/H}) = -9.35 \pm 0.06$ [21]. (There is also a severer observational limit which worsens the fitting [38].)[2] In order to explain the observed abundance of the dark matter by the Bino-like neutralino LSP based on a thermal relic scenario, the so-called stau coannihilation mechanism is required to work well [45]. This mechanism requires of order or smaller than 1% degeneracy in mass between the neutralino LSP and the stau NLSP. Due to this tight degeneracy, the stau can be long-lived [46,47] and trigger exotic nuclear reactions at the BBN era.[3] One of such exotic reactions is an internal conversion process in a bound state of the stau and ^{7}Li (^{7}Be) nuclei [10,11]. In the internal conversion process, ^{7}Li (^{7}Be) can be destroyed into lighter nuclei and their abundances are fitted to the observational ones. Therefore, in the mass-degenerate scenario, the observed abundances of the dark matter and all light elements are simultaneously realized.

[1]See also Refs. [22–29] for long-lived neutral particles.

[2]This discrepancy cannot be solved even for corrections of corresponding cross sections of nuclear reaction [39,40]. Even if we consider nonstandard astrophysical models including diffusion processes [41,42], it would be difficult to fit all of data consistently [43]. See also Ref. [44] for a recent work related to light element nucleosynthesis in accretion flows.

[3]See also Refs. [48–52] for another cosmological constraints on CHAMPs.

It is further worth examining the BBN in the mass-degenerate scenario. In general, the MSSM has sources of intergenerational mixing, though we had assumed the lepton flavor conservation in our previous works. With the intergenerational mixing, the mass eigenstates are linear combinations of flavor eigenstates. As we will discuss later in detail, the intergenerational mixing reduces the number density of the slepton via two types of processes. Success and failure of solving the ^{7}Li problem strongly depends on the number density of the slepton. Furthermore, major and minor of modifications on the light element abundances are also determined by the number density of the slepton. Thus, the modified abundances of the light elements can be predicted by the number density that is a function of mixing parameters. As a result, we can constrain the mixing parameters from the consistency between the modified and the observed abundances of the light elements.

The aim of this work is to predict the slepton mixing parameters in the mass-degenerate scenario. In this scenario, the exotic nuclear reactions catalyzed by the long-lived slepton induce both a fusion process [2] and destruction processes through internal conversions for ^{7}Li and ^{7}Be [10–12,53], and spallations for ^{4}He [21]. These processes can modify the abundance of the light elements. In fact, ^{6}Li is produced via the former process after forming a bound state of the slepton with ^{4}He. A fit by the observational abundance $^6\mathrm{Li}/^7\mathrm{Li} = 0.046 \pm 0.022$ [54] gives an allowed region in a parameter space of the mixing parameters. In addition, both deuterium (D) and tritium (T) (or ^{3}He after its decay) are produced nonthermally by the latter processes. By adopting recent observational constraints $\mathrm{D/H} = (2.80 \pm 0.20) \times 10^{-5}$ [55] and $^3\mathrm{He/D} < 0.87 + 0.27$ [56], an upper bound on the number density of the slepton is obtained as a function of its lifetime. Thus, the upper bound on the number density results in a lower bounds on the mixing parameters of the slepton. On the other hand, a sufficient number density of the slepton at the bound state formation with ^{7}Li (^{7}Be) is required for solving the ^{7}Li problem. Then, an upper bound on the mixing parameters is obtained. Hence, intriguingly, the mixing parameters of the slepton are predicted with pinpoint accuracy from both above and below in light of the current observed light element abundances.

This long-lived slepton scenario can be also examined at terrestrial experiments. For example, due to the longevity longer than *"the first three minutes of the universe,"* a small number of the long-lived slepton would decay in detectors.[4] Some of them decay into the neutralino LSP and electron (or muon) via the intergenerational mixing. Combined with the predictions on the mixing parameters using the light element abundances, we find monochromatic and diffuse spectrum in momentum distributions of the final electron (or muon). These spectrum are characteristic signatures of the mass-degenerate scenarios, and therefore we can distinguish our scenario from others.

This paper is organized as follows. In the next section, we discuss the relation between the number density of the long-lived slepton and the intergenerational mixing in the mass-degenerate scenarios. Then, we present a set of Boltzmann equations for calculating the number density as a function of the mixing parameters. In Sec. III, we analytically estimate bounds on the mixing parameters. Then, in Sec. IV, we show our numerical results. This work improves accuracy of analysis of the intergenerational mixing than the qualitative one in Ref. [53]. Allowed region on the intergenerational mixing parameter is shown from the viewpoint of observed light element abundances. In Sec. V, applying the results, we discuss collider implications of this long-lived slepton. Finally, we summarize our results and discuss the prospects.

II. INTERGENERATIONAL MIXING AND NUMBER DENSITY OF LONG-LIVED SLEPTON

Long-lived slepton leads some kinds of exotic nuclear reactions and changes light element abundances. Predicted light element abundances depend on the number density of the slepton at the BBN epoch. Interestingly, the number density is quite sensitive to the intergenerational mixing parameters of the slepton in the mass-degenerate scenarios. Therefore, in order to constrain the intergenerational mixing, the number density has to be accurately calculated as a function of the intergenerational parameters.

A calculation of the number density of the slepton consists of two steps. In the first step, the total number density of SUSY particles is calculated at a time of their chemical decoupling. After the chemical decoupling, the number density of the slepton continues to evolve till the temperature $T \simeq \delta m$ via scattering off the cosmic thermal background. Here δm is the mass difference between the slepton NLSP and the lightest neutralino LSP. Furthermore, the number of the slepton is reduced by its own natural decay. Then, as the second step, the evolution of the number density is acquired by solving relevant Boltzmann equations implementing the scatterings and the decays. We explain the calculation of the number density, and then present a set of Boltzmann equations for the calculation.

A. First step: Total number density of SUSY particles

As the first step, we calculate the total number density of SUSY particles. The total number density is equal to the relic number density of the neutralino dark matter in the current Universe, because all SUSY particles decay into

[4]Collider signatures of the long-lived slepton in the neutralino LSP scenario is studied in case that its lifetime is shorter than the beginning of BBN [57,58] in collider experiments. Measuring the lifetime and the mass difference between the slepton and the neutralino LSP, the intergenerational mixing will be determined. Combining with the other works on collider signatures of long-lived, the models can be discriminated.

the neutralino LSP in the end under the R-parity conservation. Calculation of the relic density of the neutralino dark matter in the stau-neutralino coannihilation scenario has been developed so far [45,59]. Assuming the intergenerational mixing is not so large and the main component of the slepton is stau, the calculation method is applicable for our calculation. That is, cross sections of coannihilation processes are firstly calculated, and then we solve the Boltzmann equations for sum of the number densities of SUSY particles.

After the chemical decoupling, the total number density of SUSY particles remains the value at the freeze-out. This value does not have correlation with the intergenerational mixing. This value is required as the initial condition for calculating the slepton number density as a function of the intergenerational mixing.

B. Second step: Ratio of the number density between the slepton to the neutralino

A key ingredient for constraining the mixing parameters is the evolution of the number density of the slepton after the chemical decoupling of SUSY particles.

Thermally-produced slepton decays according to its lifetime after the chemical decoupling. Hereafter we assume that the mass difference δm is smaller than the mass of tau lepton. In this situation, the decay of slepton into the neutralino LSP and a tau lepton are forbidden kinematically. In this case the slepton becomes long-lived [47].

The decay of the slepton is categorized into two types. The first one is 3- or 4-body final state processes through the stau component;

$$\begin{aligned} &\tilde{l}^{\pm} \to \tilde{\chi}_1^0 + \nu_\tau + \pi^{\pm}, \\ &\tilde{l}^{\pm} \to \tilde{\chi}_1^0 + \nu_\tau + l^{\pm} + \nu_l (l \in e, \mu). \end{aligned} \tag{1}$$

In the mass-degenerate scenario, the decay rates of these modes considerably depend on δm (see Fig. 1 in this work and Fig. 2 in Ref. [47]). The second one is 2-body final state processes through the selectron or smuon component;

$$\tilde{l}^{\pm} \to \tilde{\chi}_1^0 + l^{\pm} \qquad (l \in e, \mu). \tag{2}$$

The 2-body decay process are dominant when the mixing parameters are not very small so that the decay rates are larger than those of 3- and 4-body decays. On the contrary, when the intergenerational mixing is tiny, 3- or 4-body decay processes dominate over 2-body decay processes in spite of a tight kinematical suppression. The constraint on the mixing from these decay processes must be therefore studied carefully as both functions of δm and the mixing parameters.

Exchange processes by scattering off the thermal background also play an important role in constraining on the mixing parameters. Even after the chemical decoupling of SUSY particles, the ratio of the number density of the slepton to the neutralino continues to evolve via exchange processes,[5]

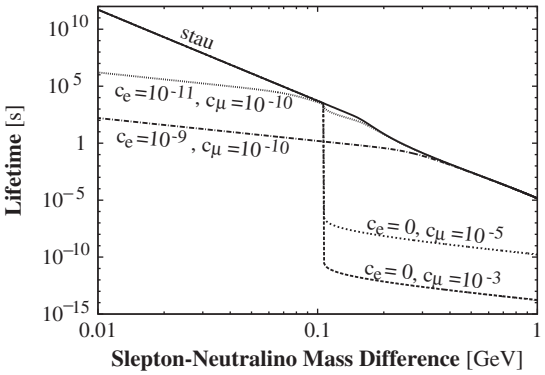

FIG. 1. Lifetime of the slepton as a function of δm for $m_{\tilde{l}} = 350$ GeV and $\sin\theta_e = 0.8$. Solid line is the lifetime of the pure stau, and others are the lifetime of slepton with each intergenerational mixing parameters.

$$\begin{aligned} &\tilde{l}^{\pm} + \gamma \leftrightarrow \tilde{\chi}_1^0 + \mu^{\pm}, \qquad \tilde{l}^{\pm} + \gamma \leftrightarrow \tilde{\chi}_1^0 + \tau^{\pm}, \\ &\tilde{\chi}_1^0 + \gamma \leftrightarrow \tilde{l}^{\pm} + l^{\mp} \qquad (l \in e, \mu). \end{aligned} \tag{3}$$

Note that the process $\tilde{l}\gamma \leftrightarrow \tilde{\chi}_1^0 e$ must not be included. The decay mode $\tilde{l} \to \tilde{\chi}_1^0 e$ is always open in the presence of the intergenerational mixing, and the process $\tilde{l}\gamma \leftrightarrow \tilde{\chi}_1^0 e$ should be counted as one of the corrective part for this decay (or inverse decay) mode with soft emission (or absorption). Thus, including the process $\tilde{l}\gamma \leftrightarrow \tilde{\chi}_1^0 e$ in addition to this decay mode results in a double counting. Similarly, when the mode $\tilde{l} \to \tilde{\chi}_1^0 \mu$ is open, then the corresponding exchange process $\tilde{l}\gamma \leftrightarrow \tilde{\chi}_1^0 \mu$ also must be taken out.

These exchange processes keep the slepton and the neutralino in kinematical equilibrium. Due to this kinematical equilibrium, the number density ratio between the slepton and the neutralino maintain the Boltzmann distributions. The number density of the slepton for a fixed δm therefore decreases as the temperature of the Universe decreases;

$$n_{\tilde{l}} = \frac{n_{\tilde{l}}}{n_{\tilde{\chi}}} \frac{n_{\tilde{\chi}}}{n_{\tilde{\chi}} + n_{\tilde{l}^+} + n_{\tilde{l}^-}} N = e^{-\delta m/T} \frac{N}{2(1 + e^{-\delta m/T})}, \tag{4}$$

where T is the temperature, and N is a sum of the densities of the slepton and the neutralino that are obtained in the first step (see Sec. II A). The kinematical equilibrium is broken when the Hubble expansion rate overwhelms the reaction rate of the exchange processes. Hence it is important to know when the Hubble expansion rate overwhelms the reaction rate. We numerically solve a set of Boltzmann equations to obtain accurate resultant number density of the slepton.

[5]Although other exchange processes exist, those contributions are negligible due to weak interactions.

C. A set of Boltzmann equations for relic number density of the slepton

Now we present a set of the Boltzmann equations to calculate the number density of the slepton as a function of the intergenerational mixing parameters. The Boltzmann equations describing evolutions of the number densities of the negatively charged slepton $n_{\tilde{l}^-}$, the positively charged slepton $n_{\tilde{l}^+}$, and the neutralino $n_{\tilde{\chi}}$ are

$$\frac{dn_{\tilde{l}^-}}{dt} + 3Hn_{\tilde{l}^-} = -\sum_{i,X,Y}[\langle\sigma' v\rangle_{iY} n_{\tilde{l}^-} n_X^{\rm eq} - \langle\sigma' v\rangle_{\tilde{l}^- X} n_i n_Y^{\rm eq}] - \sum_{X,Y,\cdots}[\langle\Gamma\rangle_{\tilde{\chi}XY\ldots} n_{\tilde{l}^-} - \langle\Gamma\rangle_{\tilde{l}^-} n_{\tilde{\chi}} n_X^{\rm eq} n_Y^{\rm eq}\cdots], \tag{5}$$

$$\frac{dn_{\tilde{l}^+}}{dt} + 3Hn_{\tilde{l}^+} = -\sum_{i,X,Y}[\langle\sigma' v\rangle_{iY} n_{\tilde{l}^+} n_X^{\rm eq} - \langle\sigma' v\rangle_{\tilde{l}^+ X} n_i n_Y^{\rm eq}] - \sum_{X,Y,\ldots}[\langle\Gamma\rangle_{\tilde{\chi}XY\ldots} n_{\tilde{l}^+} - \langle\Gamma\rangle_{\tilde{l}^+} n_{\tilde{\chi}} n_X^{\rm eq} n_Y^{\rm eq}\ldots], \tag{6}$$

$$\frac{dn_{\tilde{\chi}}}{dt} + 3Hn_{\tilde{\chi}} = -\sum_{i,X,Y}[\langle\sigma' v\rangle_{iY} n_{\tilde{\chi}} n_X^{\rm eq} - \langle\sigma' v\rangle_{\tilde{\chi}X} n_i n_Y^{\rm eq}] - \sum_{i,X,Y,\ldots}[\langle\Gamma\rangle_i n_{\tilde{\chi}} n_X^{\rm eq} n_Y^{\rm eq}\ldots - \langle\Gamma\rangle_{\tilde{\chi}XY\ldots} n_i], \tag{7}$$

where t is time and H is the Hubble parameter. In the right-hand side, $\langle\sigma' v\rangle$ is the thermal averaged cross sections of the exchange process in Eq. (3), and $\langle\Gamma\rangle$ is the thermal averaged decay rate (or inverse decay rate). The index i represents relevant SUSY particles, and indices X and Y represent the SM particles, respectively. Subscripts to both $\langle\sigma' v\rangle$ and $\langle\Gamma\rangle$ denote the final states of each process. In the equations, we assumed that the relevant SM particles are thermalized.[6]

In the presence of the intergenerational mixing, $\langle\sigma' v\rangle$ and $\langle\Gamma\rangle$ depend on the mixing parameters. Solving a set of the Boltzmann equations above, the number density of the slepton at the BBN epoch is obtained as a function of the mixing parameters. By using obtained number density, we perform the BBN calculations and predict light element abundances. Comparing them with observational values, we can constrain or predict the mixing parameters.

III. ANALYTICAL CONSTRAINT ON THE INTERGENERATIONAL MIXING

Before showing our numerical results, we give analytical estimations for bounds on the mixing parameters. We expand the lightest slepton in terms of the flavor eigenstates, $\tilde{e}$, $\tilde{\mu}$, and $\tilde{\tau}$ without the intergenerational mixing,

$$\tilde{l} = \sum_{f=e,\mu,\tau} c_f \tilde{f}, \qquad \tilde{f} = \cos\theta_f \tilde{f}_L + \sin\theta_f \tilde{f}_R, \tag{8}$$

where $\tilde{f}_L$ and $\tilde{f}_R$ are left-handed and right-handed sleptons, and θ_f are the mixing angles of these sleptons, respectively. The coefficients c_e, c_μ, and c_τ are the mixing parameters. These parameters are in ranges from zero to unity and satisfy the relation $c_e^2 + c_\mu^2 + c_\tau^2 = 1$. In this work, we assume c_e, c_μ, and c_τ to be real and positive parameters for simplicity.

These mixing parameters are constrained from above by two requirements. The first requirement is the sufficient longevity of the slepton, and the second one is the sufficient number density at the moment of decoupling from the exchange processes. For the first requirement, the lifetime of the slepton must be longer than $\mathcal{O}(10^3$ s) to solve the ^{7}Li problem. The slepton with this lifetime can form a bound state with ^{7}Li and ^{7}Be and destroy these nuclei via the internal conversion processes [10,11]. The lifetime is depicted as a function of δm in Fig. 1 for $m_{\tilde{l}} = 350$ GeV and $\sin\theta_e = \sin\theta_\mu = 0.8$. A curve labeled "stau" is the lifetime for a pure stau, and other curves are the lifetime for the slepton with the mixing parameters labeled near the curves. The lifetime varies by a few order of magnitudes as δm and $c_{e,\mu}$ vary. Due to the kinematical thresholds for the decays, dependence on both c_e and c_μ is different for $\delta m > m_\mu$ or $\delta m < m_\mu$. Therefore, the lifetime should be studied in each δm region to obtain bounds on the mixing parameters.

To obtain the bounds analytically, we consider two simple cases in which either $c_e = 0$ or $c_\mu = 0$ for simplicity. For $c_\mu = 0$ case, the slepton decays into an electron and the lightest neutralino (2-body decay). Then the lifetime of the slepton is approximately given by

$$\tau_{\tilde{l}}(\tilde{l} \to \tilde{\chi}_1^0 + e) \simeq \frac{8\pi}{g^2 \tan^2\theta_W} \frac{m_{\tilde{l}}}{(\delta m)^2} \frac{1}{\cos^2\theta_e + 4\sin^2\theta_e} \frac{1}{c_e^2}, \tag{9}$$

where $m_{\tilde{l}}$ is the mass of the slepton. By inserting $\cos\theta_e = 0.6$ for a reference value, the lifetime is expressed as

$$\tau_{\tilde{l}}(\tilde{l} \to \tilde{\chi}_1^0 + e) \simeq 1.34 \times 10^3 \left[\frac{m_{\tilde{l}}}{300\ \text{GeV}}\right]\left[\frac{0.1\ \text{GeV}}{\delta m}\right]^2 \left[\frac{4 - 3(0.6)^2}{4 - 3\cos^2\theta_e}\right] \times \left[\frac{10^{-10.5}}{c_e}\right]^2 \text{s}.$$

Requiring $\tau_{\tilde{l}} \geq \mathcal{O}(10^3$ s), we obtain the bound on the selectron component, $c_e \lesssim 3.2 \times 10^{-11}$ for $\delta m = 0.1$ and $m_{\tilde{l}} = 300$ GeV. Similarly, for $c_e = 0$ case, the lifetime is approximately given as

[6] Vability of this assumption is checked in Ref. [53].

$$\tau_{\tilde{l}}(\tilde{l} \to \tilde{\chi}_1^0 + \mu) \simeq 10^3 \left[\frac{10^{-10.5}}{c_\mu}\right]^2 \left[\frac{0.12\ \text{GeV}}{\delta m}\right]^2 \left[\frac{m_{\tilde{l}}}{300\ \text{GeV}}\right] \times \left(1 - \frac{25}{36}\left[\frac{0.12\ \text{GeV}}{\delta m}\right]^2\right)^{-1/2} \text{s}, \quad (10)$$

where $\cos\theta_\mu = 0.6$ is used. From Eq. (10), the upper bound on c_μ is obtained as 3.2×10^{-11} for $\delta m = 0.1$ and $m_{\tilde{l}} = 300$ GeV.

We can derive another upper bounds on the mixing parameters from the second requirement that the number density should be sufficient at the decoupling time from the exchange processes to destroy the ^{7}Li and ^{7}Be nuclei. Omitting smuon component again, the exchange processes are $\tilde{l}e \leftrightarrow \tilde{\chi}_1^0\gamma$ and $\tilde{l}\tau \leftrightarrow \tilde{\chi}_1^0\gamma$ through selectron and stau component. The former exchange process keeps working even after the freeze-out of the latter process. This is because densities of electron and photon are still quite large in thermal bath for $T \lesssim m_\tau$. Then, as explained in the previous section, the slepton number density continues to decrease. The reaction rate with the electron is proportional to c_e^2. Hence the larger the mixing is, the more the number density decreases. The reaction rate of $\tilde{l}e \leftrightarrow \tilde{\chi}_1^0\gamma$ must be suppressed to ensure a sufficient number density of the slepton. The bound on c_e is estimated by comparing this reaction rate with that of processes with tau.

In the absence of the intergenerational mixing or pure stau case, freeze-out of the exchange processes ($\tilde{l}^\pm\gamma \leftrightarrow \tilde{\chi}_1^0\tau^\pm$ and $\tilde{\chi}_1^0\gamma \leftrightarrow \tilde{l}^\pm\tau^\mp$) occurs at $T \simeq 70$ MeV, and is almost independent of both δm and $m_{\tilde{l}}$ [53]. Then the number density of the slepton manages to be a sufficient amount. This fact suggests that the reaction rate of $\tilde{l}e \leftrightarrow \tilde{\chi}_1^0\gamma$ must be smaller than that of the processes in the absence of the intergenerational mixing at $T = 70$ MeV. Parametrizing the cross section of this process as $\langle\sigma' v\rangle_e = c_e^2\langle\sigma' v\rangle_\tau$, the ratio of these reaction rates at $T = 70$ MeV is given by

$$\frac{\langle\sigma' v\rangle_e Y_{\tilde{l}} Y_e}{\langle\sigma' v\rangle_\tau Y_{\tilde{l}} Y_\tau} \simeq (1.08 \times 10^9) c_e^2, \quad (11)$$

at $Y_{\tilde{l}}$ and $Y_{e,\tau}$ are the yield value of the slepton and electron/tau, respectively. The mixing parameter c_e is therefore required to be $\lesssim 3 \times 10^{-5}$. For $c_e = 0$ case, the reaction rate of the process $\tilde{l}\mu \leftrightarrow \tilde{\chi}_1^0\gamma$ is compared with that without the mixing. Parametrizing the cross section of the process as $\langle\sigma' v\rangle_\mu = c_\mu^2\langle\sigma' v\rangle_\tau$, the ratio of the reaction rates is given by

$$\frac{\langle\sigma' v\rangle_\mu Y_{\tilde{l}} Y_\mu}{\langle\sigma' v\rangle_\tau Y_{\tilde{l}} Y_\tau} \simeq (9.93 \times 10^7) c_\mu^2, \quad (12)$$

at temperature $T = 70$ MeV. From Eq. (12), c_μ must to be smaller than 10^{-4}.

As we will see later, we can constrain c_e from below by the relic abundance of light elements. Thus we will get an allowed region for c_e.

IV. NUMERICAL RESULTS

We are now in a position to numerically search for an allowed region of the slepton mixing parameters. First, we see that the upper bounds on c_e and c_μ obtained in the previous section are in a good agreement with numerical analysis. Then, we numerically compute reaction networks of light elements including the exotic nuclear reactions, and find parameter regions as a function of δm allowed by the observational light element abundances.

A. Constraint on slepton intergenerational mixing

First, we show bounds on the mixing parameter c_μ for $\delta m < m_\mu$. Based on previous works [11], we fix $Y_{\tilde{l}} = 2 \times 10^{-13}$ for the sufficient number density to solve the ^{7}Li problem.

Figure 2 shows the temperature evolution of the yield values of the slepton for each values of c_μ. The value of c_μ is shown near corresponding curves. From top to bottom panels, the mass differences are taken to be $\delta m = 20$, 60, and 100 MeV, respectively. The curves tagged by stau represent the yield values without the mixing, and the curves tagged by "Equilibrium" are the yield values of the slepton in kinetic equilibrium. In shaded region, number density of the slepton is insufficient to solve the ^{7}Li problem. In each panel, we took $c_e = 0$, because bound on c_e is $c_e \lesssim 10^{-10}$ and hence contributions of c_e are negligible when the exchange processes are still working. As is expected, larger value of c_μ keeps yield values of the slepton to be in kinetic equilibrium and leads smaller number densities of the slepton.

The bound on $c_\mu \lesssim 5 \times 10^{-5}$ for $\delta m = 20$ MeV [Fig. 2(a)] accurately reproduces our estimation in the previous section. For larger δm, the bounds on c_μ become more stringent; $c_\mu \lesssim 2 \times 10^{-6}$ for $\delta m = 60$ MeV [Fig. 2(b)], and $c_\mu \lesssim 2 \times 10^{-7}$ for $\delta m = 100$ MeV [Fig. 2(c)]. This is understood as follows. The cross sections for the processes (3) are not so dependent on δm for $\delta m < m_\mu$. They are more dependent on the muon number density and hence the temperature. It means that the decoupling temperature of these processes are almost same as long as c_μ is same. Then to have a sufficient yield, these processes must decouple earlier for larger mass difference. See Eq. (4). Thus less intergenarational mixing is allowed for larger mass difference.

In the case of $\delta m \geq m_\mu$, more stringent bounds on c_μ are derived from the requirement on lifetimes of the slepton. To solve the ^{7}Li problem, the bound states of the slepton and ^{7}Be (^{7}Li) have to be sufficiently formed. This formation requires the lifetime of the slepton to be at least 1000s, preferably 2000s (see Fig. 1 in Ref. [12]).

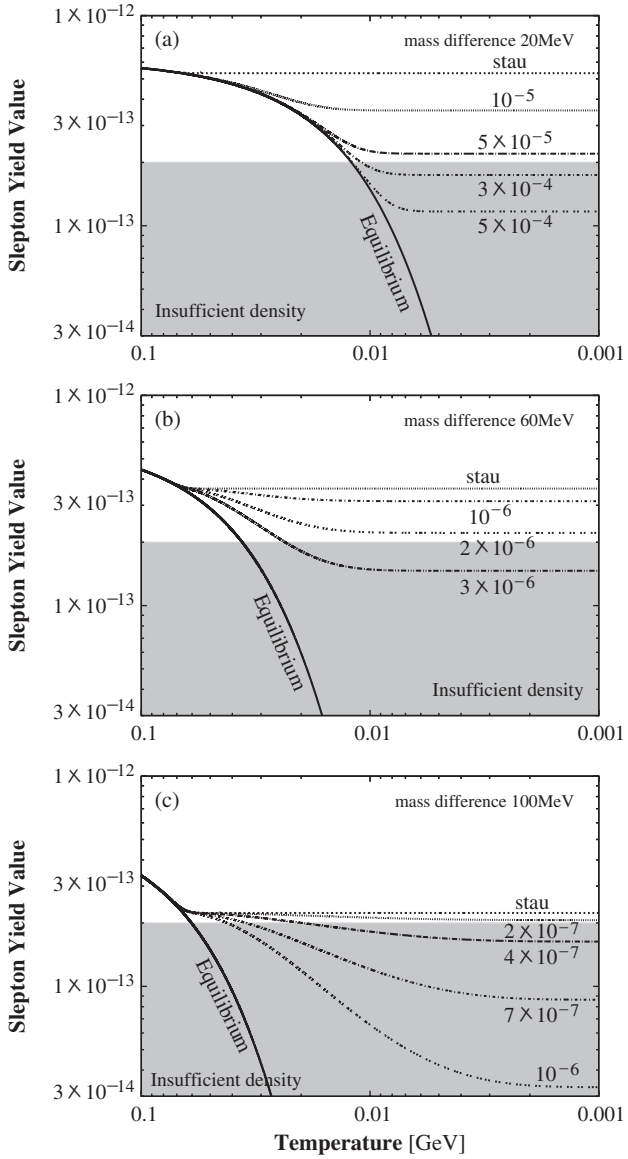

FIG. 2. Evolution of slepton yield values $Y_{\tilde{l}}$ for each smuon component c_μ, which values are attached on corresponding curve. Curves tagged by stau are yield values of pure stau, and curves tagged by Equilibrium are yield values of the slepton in kinetic equilibrium. In shaded region, number density of the slepton is insufficient for solving the ^{7}Li problem.

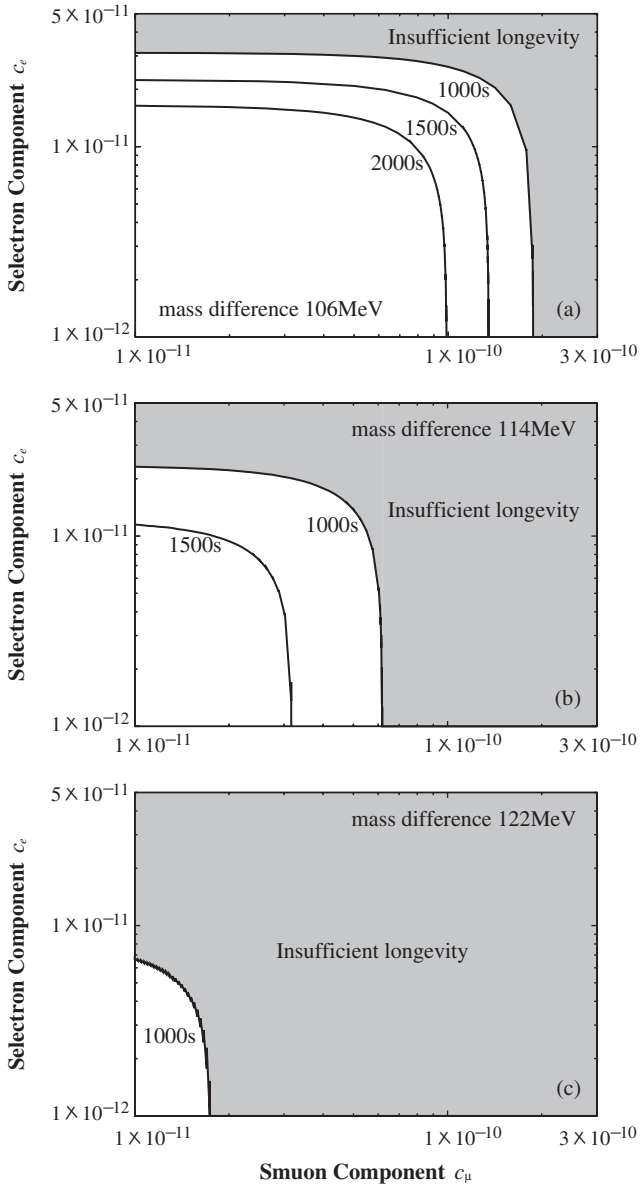

FIG. 3. Bounds both on c_μ and c_e for $\delta m \geq m_\mu$. Shaded region is disfavored in light of solving the ^{7}Li problem, wherein the slepton decays before forming a bound state with ^{7}Be and ^{7}Li.

Figure 3 shows bounds both on c_μ and c_e for $\delta m = 106$, 114, 122 MeV, respectively. Values near each curves are the lifetime of the slepton. In shaded region, the lifetime of the slepton is shorter than 1000s, and hence the parameters in this region are excluded. In left-side and down-side region in each panel, 4-body decay process is dominant because the mixing parameters are so small. This result is consistent with the result in Fig. 1. The upper bounds on c_μ obtained here are $c_\mu \lesssim 2\times10^{-10}$ for $\delta m = 106$ MeV, which is just above the threshold of the decay of the slepton into a muon, and $c_\mu \lesssim 6\times10^{-11}$ for $\delta m = 114$ MeV, $c_\mu \lesssim 2\times10^{-11}$ for $\delta m = 122$ MeV.

B. Allowed regions by big-bang nucleosynthesis

By numerically solving the Boltzmann equations, we obtain time evolutions of the bound states such as (^{4}He$\tilde{l}^-$), (^{7}Li$\tilde{l}^-$), and (^{7}Be$\tilde{l}^-$) including charge-exchange reactions [16,51]. Once those bound states are formed, the elements are immediately destroyed through internal conversion processes for ^{7}Li and ^{7}Be, and spallation processes for ^{4}He, induced by bound-state effects [10–12,53]. Then by solving coupled equations of the reactions including those nonstandard processes, we can obtain final abundances of the light elements. We adopt a value of baryon to photon ratio $\eta = (6.225 \pm 0.170)\times10^{-10}$ (68% C.L.) which was reported by the WMAP satellite [60].

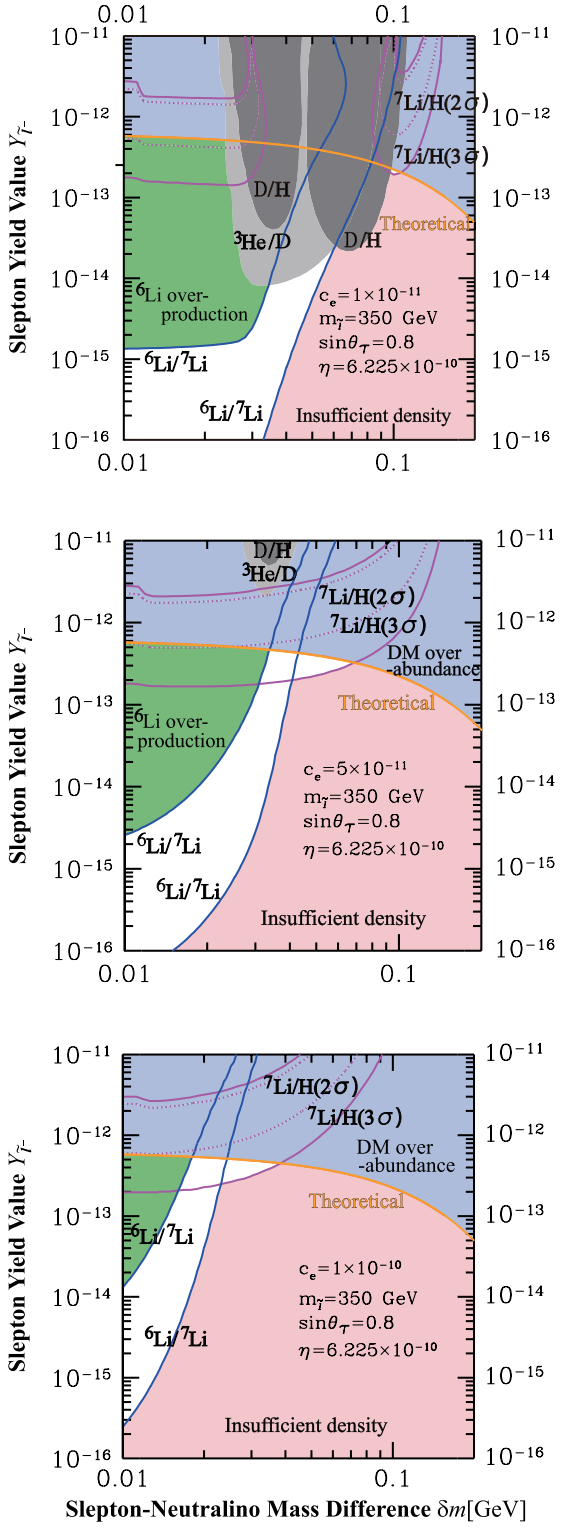

FIG. 4 (color online). Allowed regions by observational light element abundances in $\delta m - Y_{\tilde{l}^-}$ planes in cases of $c_e = 10^{-11}$ (top panel), 5×10^{-11} (middle panel), and 10^{-10} (bottom panel). The lines of the constraints are plotted for D/H, ^{3}He/D, and ^{6}Li/^{7}Li at 2σ. An exception is ^{7}Li/H whose constraints are denoted by both dotted lines at 2σ, and solid lines at 3σ. The theoretical curve of the relic abundance is also plotted as a thick solid line.

^{7}Be and ^{7}Li are efficiently destroyed through internal conversion processes $(^7\mathrm{Be}\tilde{l}^-) \to {}^7\mathrm{Li} + \nu_l + \tilde{\chi}_1^0$ with a following standard process $^7\mathrm{Li} + p \to {}^4\mathrm{He} + {}^4\mathrm{He}$, or another subdominant internal conversion process $(^7\mathrm{Li}\tilde{l}^-) \to {}^7\mathrm{He} + \nu_l + \tilde{\chi}^0$. Then we can compare this theoretical value with the observational abundance. It is notable that most of primordial ^{7}Li is produced by primordial ^{7}Be through its electron capture at a much later time for the adopted value of η. We have also included the production process of ^{6}Li through the bound-state effect $(^4\mathrm{He}\tilde{l}^-) + \mathrm{D} \to {}^6\mathrm{Li} + \tilde{l}^-$ [2,9].

On the other hand, D and ^{3}He are nonthermally produced by the ^{4}He spallation processes $(^4\mathrm{He}\tilde{l}^-) \to \mathrm{T} + n + \tilde{\chi}_1^0 + \nu_l$, $(^4\mathrm{He}\tilde{l}^-) \to \mathrm{D} + 2n + \tilde{\chi}_1^0 + \nu_l$, $(^4\mathrm{He}\tilde{l}^-) \to p + 3n + \tilde{\chi}_1^0 + \nu_l$, and subsequent standard processes for n and p [53]. Note that ^{7}Li or ^{7}Be is also secondarily produced by those nonthermally-produced energetic T and ^{3}He, which may worsen the ^{7}Li problem partly in the parameter spaces.

In Fig. 4 we plot regions allowed by observational light element abundances in δm-$Y_{\tilde{l}^-}$ planes in cases of $c_e = 10^{-11}$ (top panel), 5×10^{-11} (middle panel), and 10^{-10} (bottom panel). Lines of the constraints are plotted for D/H, ^{3}He/D, and ^{6}Li/^{7}Li at 2σ. An exception is ^{7}Li/H whose lines are denoted by both dotted lines at 2σ, and solid lines at 3σ. The theoretical curve of the relic abundance is also plotted as a thick solid line. For simplicity, here we have assumed $c_\mu = 0$.

In Fig. 5, we also plot allowed regions in the δm-c_e plane by using the theoretical value of the relic abundance for the negatively charged slepton at each point of the plane. Each panel is plotted with same parameters.

The region on the bottom-left side of thick dotted line is free from ^{7}Li problem at 3σ, and the region on the other side of the line is excluded due to insufficient density of the slepton. The regions between the two blue solid lines are allowed for ^{6}Li/^{7}Li at 2σ. The ^{4}He spallation processes exclude the shadowed, light shadowed, and dark shadowed regions due to over-productions of D/H, ^{3}He/D, and ^{7}Li/H at 2σ, respectively. The region on the bottom-left side of the left blue solid line is excluded by ^{6}Li over-production. Thus the white region in top panel (bottom panel) is the parameter space which is consistent with all of observational light element abundances including ^{7}Li (both ^{7}Li and ^{6}Li).

V. COLLIDER SIGNATURE

Finally, we have a short discussion on collider signatures of the long-lived slepton. The long-lived sleptons stopped in a detector decay into 2-body final state $(\tilde{l} \to \tilde{\chi}_1^0 e)$ and 4-body final state $(\tilde{l} \to \tilde{\chi}_1^0 \nu_\tau e \bar{\nu}_e)$. From the results in previous section, we can predict the ratio of the number of events between these decays. One of the way to confirm our scenario is to search for double peaks in electron

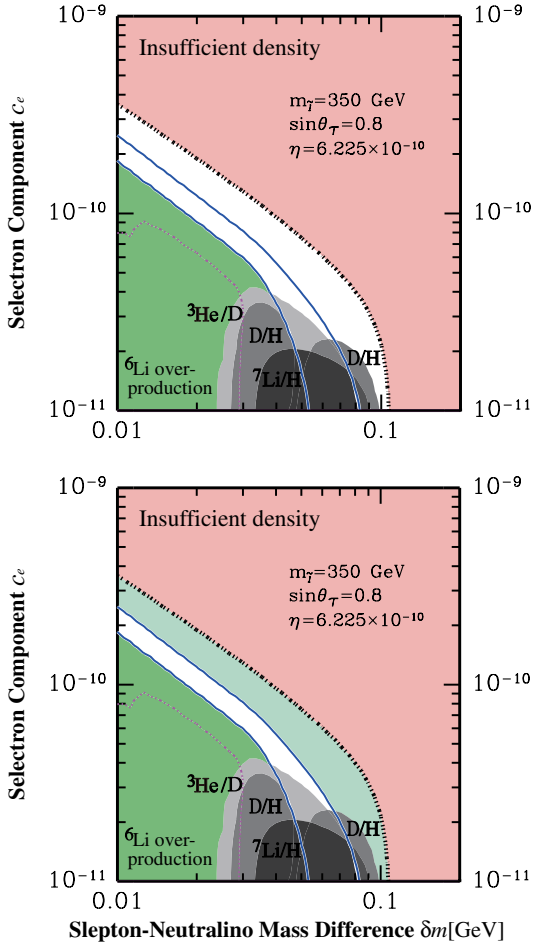

FIG. 5 (color online). Allowed region in the $\delta m - c_e$ plane. Each panel is plotted with same parameters. The region on the bottom-left side of thick dotted line is free from ^{7}Li problem at 3σ. The regions between two blue solid lines are allowed for ^{6}Li/^{7}Li. The ^{4}He spallation processes exclude shadowed, light shadowed, and dark shadowed regions due to over-productions of D/H, ^{3}He/D, and ^{7}Li/H, respectively. The region on the bottom-left side of left blue solid line is excluded by ^{6}Li over-production. The white region in top panel (bottom panel) is the parameter space which is consistent with all of observational light element abundances including ^{7}Li (both ^{7}Li and ^{6}Li).

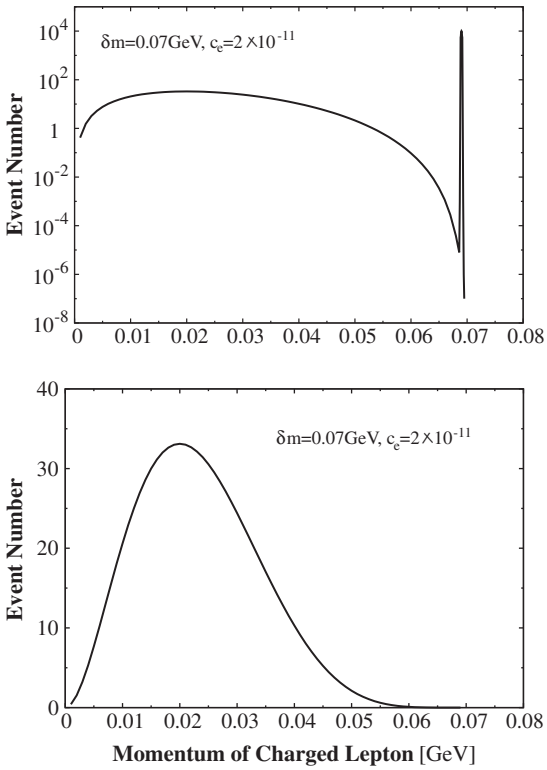

FIG. 6. Event number distribution of the decay of the long-lived slepton as a function of momentum of final state electron. We assumed detector resolution to be 1 MeV, and normalized number of 2-body decay to 10^4 events in a bin.

momentum distribution in the decay of the long-lived slepton, and count the event number ratio.

Figure 6 shows expected event distributions of the decay as a function of electron momentum. The event distributions of both 2-body and 4-body decays are plotted in log scale in top panel, and bottom panel plots the distribution of only 4-body decay in linear scale. We took $m_{\tilde{l}} = 350$ GeV, $\delta m = 0.07$ GeV, $c_e = 2 \times 10^{-11}$, and $c_\mu = 0$. This parameter set is found in allowed region (see Fig. 5). We assumed detector resolution to be 1 MeV, and normalized number of 2-body decay to 10^4 events in a bin. One can see in the top panel that there is a peak at the momentum of 0.07 GeV. The peak corresponds to 2-body decay because the momentum is the same value of δm. On the other hand, in the bottom panel, one can see that 4-body decay also shows a peak around 0.2 GeV. This peak is broader than that of the 2-body decay. Number of event of 2-body decay is almost 100 times more than peak number of 4-body decay. Thus, the event distribution shows a double peak structure, and this is a characteristic feature for mass-degenerate scenario.

If exotic charged tracks of long-lived particle are discovered, new facility may be constructed with higher accumulation efficiency and high momentum resolution. Discovery of unique signatures of the decay in addition to charged tracks of long-lived particle will be a strong evidence of this scenario.

VI. SUMMARY

We have considered a scenario of the MSSM where the slepton NLSP is long-lived due to a small mass difference between the NLSP and the neutralino LSP, and studied the effects of the intergenerational mixing of sleptons on big-bang nucleosynthesis. In this scenario, the so-called internal conversion processes occurs in the bound states between the slepton NLSP and light nuclei in BBN. Then, the ^{7}Li and ^{6}Li problems can be solved

simultaneously when the slepton NLSP is enough long-lived and its number density is sufficient at the era of BBN. We have analyzed the yield value and the lifetime of the slepton with the intergenerational mixing as well as the relic abundances of the light elements including the internal conversion processes in BBN.

In Sec. III, we have calculated the yield value and the lifetime of the slepton NLSP and derived upper bounds on the mixing parameters c_μ. The upper bounds are obtained by requiring the yield value and the lifetime to be $Y_{\tilde{l}} \sim 2 \times 10^{-13}$ and $\tau_{\tilde{l}} \geq 10^3$ sec. to solve the ^{7}Li problem. In the case of $\delta m < m_\mu$, the upper bounds are given as $c_\mu \leq 5 \times 10^{-5}$, 2×10^{-6}, and 2×10^{-7} for $\delta m = 20$, 60, and 100 MeV, respectively. On the other hand, in the case of $\delta m > m_\mu$, the upper bounds, $c_\mu \leq 2 \times 10^{-10}$, 6×10^{-11}, and 2×10^{-11}, are given for $\delta m = 106$, 114, and 122 MeV, respectively.

We have also analyzed the the relic abundances of the light elements by solving the Boltzmann equations taking into account all the exotic processes listed in Sec. IV. We derived an allowed region on c_e by adopting 2σ uncertainties for D/H, ^{3}He/D, and ^{6}Li/^{7}Li, and 2σ and 3σ uncertainty for ^{7}Li/H. We found that, assuming $c_\mu = 0$, the ^{7}Li and ^{6}Li problems can be solved simultaneously in the range of $2 \times 10^{-11} \leq c_e \leq 2 \times 10^{-9}$. These results are consistent with the estimations given in Sec. II.

In the end, we have discussed the decays of the slepton in a case of $\delta m = 0.07$ GeV and $c_e = 2 \times 10^{-11}$ as an illustrating example. We found that the 2-body decay shows a line spectrum at the momentum of an outgoing electron close to δm while the 4-body decay shows a broad peak in the momentum distribution. The expected number of events for 2-body decay is 100 times larger than that for 4-body decay. These features as well as heavy charged tracks are unique in the degenerate-mass scenario. In the case that lifetime of the long-lived slepton is 10^3 sec, even present working detectors can stop the produced long-lived sleptons and accumulate $\sim$0.5% of them approximately [61] (some other ideas for stopping long-lived charged particles have been proposed so far in Refs. [62–64]). Discovery of the charged tracks may promote construction of new facility with higher accumulation efficiency and momentum resolution. The discovery of characteristic features, the double peaks and the charged tracks, will be a strong evidence of our scenario.

ACKNOWLEDGMENTS

This work was supported in part by the Grant-in-Aid for the Ministry of Education, Culture, Sports, Science, and Technology, Government of Japan, Grants No. 21111006, No. 22244030, No. 23540327 (K. K.), No. 23740190 (T. S.), No. 24340044 (J. S.), and No. 23740208 (M. Y.).

[1] M. Fairbairn, A. C. Kraan, D. A. Milstead, T. Sjostrand, P. Z. Skands, and T. Sloan, Phys. Rep. **438**, 1 (2007), and references therein.
[2] M. Pospelov, Phys. Rev. Lett. **98**, 231301 (2007).
[3] K. Kohri and F. Takayama, Phys. Rev. D **76**, 063507 (2007).
[4] M. Kaplinghat and A. Rajaraman, Phys. Rev. D **74**, 103004 (2006).
[5] R. H. Cyburt, J. R. Ellis, B. D. Fields, K. A. Olive, and V. C. Spanos, J. Cosmol. Astropart. Phys. 11 (2006) 014.
[6] M. Kawasaki, K. Kohri, and T. Moroi, Phys. Lett. B **649**, 436 (2007).
[7] M. Kawasaki, K. Kohri, T. Moroi, and A. Yotsuyanagi, Phys. Rev. D **78**, 065011 (2008).
[8] F. D. Steffen, AIP Conf. Proc. **903**, 595 (2007).
[9] K. Hamaguchi, T. Hatsuda, M. Kamimura, Y. Kino, and T. T. Yanagida, Phys. Lett. B **650**, 268 (2007).
[10] C. Bird, K. Koopmans, and M. Pospelov, Phys. Rev. D **78**, 083010 (2008).
[11] T. Jittoh, K. Kohri, M. Koike, J. Sato, T. Shimomura, and M. Yamanaka, Phys. Rev. D **76**, 125023 (2007).
[12] T. Jittoh, K. Kohri, M. Koike, J. Sato, T. Shimomura, and M. Yamanaka, Phys. Rev. D **78**, 055007 (2008).
[13] K. Jedamzik, Phys. Rev. D **77**, 063524 (2008).
[14] J. Pradler and F. D. Steffen, Phys. Lett. B **666**, 181 (2008).
[15] M. Pospelov, J. Pradler, and F. D. Steffen, J. Cosmol. Astropart. Phys. 11 (2008) 020.
[16] M. Kamimura, Y. Kino, and E. Hiyama, Prog. Theor. Phys. **121**, 1059 (2009).
[17] M. Kusakabe, T. Kajino, T. Yoshida, T. Shima, Y. Nagai, and T. Kii, Phys. Rev. D **79**, 123513 (2009).
[18] S. Bailly, K. Jedamzik, and G. Moultaka, Phys. Rev. D **80**, 063509 (2009).
[19] S. Bailly, K. Y. Choi, K. Jedamzik, and L. Roszkowski, J. High Energy Phys. 05 (2009) 103.
[20] M. Kusakabe, T. Kajino, T. Yoshida, and G. J. Mathews, Phys. Rev. D **81**, 083521 (2010).
[21] T. Jittoh, K. Kohri, M. Koike, J. Sato, K. Sugai, M. Yamanaka, and K. Yazaki, Phys. Rev. D **84**, 035008 (2011).
[22] K. Jedamzik, Phys. Rev. D **70**, 063524 (2004).
[23] M. Kawasaki, K. Kohri, and T. Moroi, Phys. Lett. B **625**, 7 (2005).
[24] M. Kawasaki, K. Kohri, and T. Moroi, Phys. Rev. D **71**, 083502 (2005).
[25] D. Cumberbatch, K. Ichikawa, M. Kawasaki, K. Kohri, J. Silk, and G. D. Starkman, Phys. Rev. D **76**, 123005 (2007).
[26] K. Kohri and Y. Santoso, Phys. Rev. D **79**, 043514 (2009).
[27] R. H. Cyburt, J. Ellis, B. D. Fields, F. Luo, K. A. Olive, and V. C. Spanos, J. Cosmol. Astropart. Phys. 10 (2009) 021.

[28] M. Pospelov and J. Pradler, Phys. Rev. D **82**, 103514 (2010).
[29] M. Kawasaki and M. Kusakabe, Phys. Rev. D **83**, 055011 (2011).
[30] J. R. Ellis, K. A. Olive, Y. Santoso, and V. C. Spanos, Phys. Lett. B **588**, 7 (2004).
[31] D. G. Cerdeno, K.-Y. Choi, K. Jedamzik, L. Roszkowski, and R. Ruiz de Austri, J. Cosmol. Astropart. Phys. 06 (2006) 005.
[32] F. D. Steffen, J. Cosmol. Astropart. Phys. 09 (2006) 001.
[33] L. Covi, L. Roszkowski, R. Ruiz de Austri, and M. Small, J. High Energy Phys. 06 (2004) 003.
[34] A. Freitas, F. D. Steffen, N. Tajuddin, and D. Wyler, J. High Energy Phys. 06 (2011) 036.
[35] E. J. Chun, H. B. Kim, K. Kohri, and D. H. Lyth, J. High Energy Phys. 03 (2008) 061.
[36] R. H. Cyburt, B. D. Fields, and K. A. Olive, J. Cosmol. Astropart. Phys. 11 (2008) 012.
[37] J. Melendez and I. Ramirez, Astrophys. J. **615**, L33 (2004).
[38] P. Bonifacio *et al.*, Astron. Astrophys. **462**, 851 (2007).
[39] R. H. Cyburt, B. D. Fields, and K. A. Olive, Phys. Rev. D **69**, 123519 (2004).
[40] C. Angulo *et al.*, Astrophys. J. **630**, L105 (2005).
[41] O. Richard, G. Michaud, and J. Richer, Astrophys. J. **619**, 538 (2005).
[42] A. J. Korn, F. Grundahl, O. Richard, P. S. Barklem, L. Mashonkina, R. Collet, N. Piskunov, and B. Gustafsson, Nature (London) **442**, 657 (2006).
[43] K. Lind, F. Primas, C. Charbonnel, F. Grundahl, and M. Asplund, arXiv:0906.2876.
[44] F. Iocco and M. Pato, Phys. Rev. Lett. **109**, 021102 (2012).
[45] K. Griest and D. Seckel, Phys. Rev. D **43**, 3191 (1991).
[46] S. Profumo, K. Sigurdson, P. Ullio, and M. Kamionkowski, Phys. Rev. D **71**, 023518 (2005).
[47] T. Jittoh, J. Sato, T. Shimomura, and M. Yamanaka, Phys. Rev. D **73**, 055009 (2006).
[48] K. Sigurdson and M. Kamionkowski, Phys. Rev. Lett. **92**, 171302 (2004).
[49] J. Hisano, K. T. Inoue, and T. Takahashi, Phys. Lett. B **643**, 141 (2006).
[50] F. Borzumati, T. Bringmann, and P. Ullio, Phys. Rev. D **77**, 063514 (2008).
[51] K. Kohri and T. Takahashi, Phys. Lett. B **682**, 337 (2010).
[52] L. Chuzhoy and E. W. Kolb, J. Cosmol. Astropart. Phys. 07 (2009) 014.
[53] T. Jittoh, K. Kohri, M. Koike, J. Sato, T. Shimomura, and M. Yamanaka, Phys. Rev. D **82**, 115030 (2010).
[54] M. Asplund, D. L. Lambert, P. E. Nissen, F. Primas, and V. V. Smith, Astrophys. J. **644**, 229 (2006).
[55] M. Pettini, B. J. Zych, M. T. Murphy, A. Lewis, and C. C. Steidel, Mon. Not. R. Astron. Soc. **391**, 1499 (2008).
[56] J. Geiss and G. Gloeckler, Space Sci. Rev. **106**, 3 (2003).
[57] S. Kaneko, J. Sato, T. Shimomura, O. Vives, and M. Yamanaka, Phys. Rev. D **78**, 116013 (2008).
[58] S. Kaneko, H. Saito, J. Sato, T. Shimomura, O. Vives, and M. Yamanaka, Phys. Rev. D **83**, 115005 (2011).
[59] J. Edsjo and P. Gondolo, Phys. Rev. D **56**, 1879 (1997).
[60] E. Komatsu *et al.* (WMAP Collaboration), Astrophys. J. Suppl. Ser. **192**, 18 (2011).
[61] S. Asai, K. Hamaguchi, and S. Shirai, Phys. Rev. Lett. **103**, 141803 (2009).
[62] K. Hamaguchi, Y. Kuno, T. Nakaya, and M. M. Nojiri, Phys. Rev. D **70**, 115007 (2004).
[63] J. L. Feng and B. T. Smith, Phys. Rev. D **71**, 015004 (2005); **71**, 019904 (2005).
[64] A. De Roeck, J. R. Ellis, F. Gianotti, F. Moortgat, K. A. Olive, and L. Pape, Eur. Phys. J. C **49**, 1041 (2007).